URSI GASS 2020, Rome, Italy, 29 August - 5 September 2020

Recent Development of Microwave and Millimeter-Wave Dual-Circularly-Polarized Arrays

Zhi Hao Jiang*(1), Xiao-Wei Zhu(1), and Wei Hong(1)
(1) State Key Laboratory of Millimeter-Waves, School of Information Science and Engineering, Southeast University, Nanjing, 210096, China.
zhihao.jiang@seu.edu.cn

Abstract

This paper presents a summary of recent development of dual-circularly-polarized arrays, including antenna arrays and reflect-/transmit-arrays, at microwave and millimeter-wave frequencies. They are enabled by utilizing both the rotational phase due to element rotation and dynamic phase provided by phase shifters or resonator with different sizes. The design and experimental results of several illustrative dual-circularly-polarized antenna array and reflect/transmit-array examples are shown.

1 Introduction

Circularly-polarized (CP) radiating devices [1] are highly useful in communication and radar systems particularly for space applications [2] and/or in scenarios where device misalignment induced polarization mismatch is required to be mitigated [3]. In general, to form low-profile and planarized CP radiating devices with a high gain, antenna arrays with guided-wave feeding networks [4] or reflect/transmit-arrays (RAs/TAs) with quasi-optical power dividing architectures [5] can be utilized. For antenna arrays, the most straightforward approach is to employ an array of identical CP elements with the same element orientation [6]. However, this often leads to a narrow axial ratio (AR) bandwidth. Alternatively, linearly-polarized (LP) elements can be used to form CP radiation by using a sequential rotation technique, which can provide a broad AR bandwidth but only a single handedness with a single feeding network [7]. Regarding RAs/TAs, isotropic dynamic phase cells [8] or anisotropic rotational phase cells [9] with CP feeds have been investigated. However, most of these CP antenna arrays and RAs/TAs cannot support dual-CP functionality, which is beneficial for increasing the data transmission rate. In this paper, several dual-CP antenna arrays and RAs/TAs achieved by utilizing both rotational and dynamic phases are presented.

2 Dual-CP Antenna Arrays

Dual-CP antenna arrays with two ports were investigated based on sequential rotation technique and integrated feeding networks. As shown in Figure 1(a), the dual-port dual-CP antenna array is comprised by four LP sub-arrays, each containing four radiating elements of four patches. Each of the four sub-arrays is rotated with a successive angle increasement of 90°. In order to achieve dual-CP radiation in the same frequency band, the feeding phases for the 4 sub-arrays should be 0°/-90°/-180°/-270° and 0°/90°/180°/270° for right- and left-handed CP (RHCP and LHCP) radiation, respectively. An eight-port feeding network based on substrate integrated waveguide circuit components was designed accordingly. Only two of its four input ports were utilized, with one port generating a RHCP beam and another port exciting a LHCP beam. The fabricated prototype owns a wide bandwidth of around 8.9%, high isolation of more than 19 dB, a low profile of less than $0.1\lambda_0$, and orthogonal polarization discrimination of higher than 25 dB (see Figure 1(b)) [10].

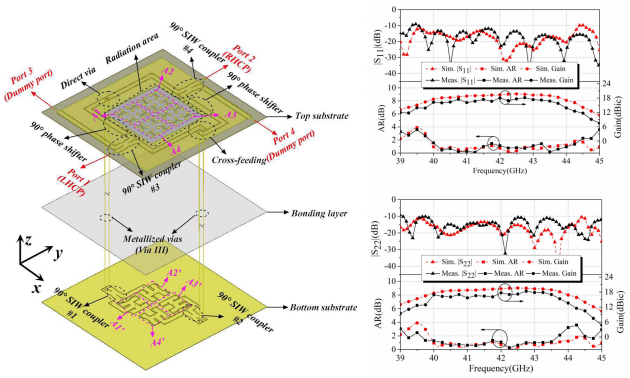

(a) (b)

Figure 1. (a) Configuration of the dual-port dual-CP *Q*-band antenna array. (b) Simulated and measured port reflection, AR, and gain of the LHCP and RHCP ports.

In many space communication systems, the RHCP and LHCP beams, one for uplink and the other for downlink, should operate at different frequency bands. To achieve such a property, a more advanced dual-CP antenna array with self-diplexing function was developed. As shown in Figure 2(a), the antenna array is composed of 4 sub-arrays. In each sub-array, the four patch elements are sequentially rotated. Particularly, each patch was cut by a slot at the center for increasing the isolation between the two bands, where both of its two orthogonal LP modes are utilized. A multilayer microstrip feeding network was synthesized, which provides sequential feeding phases for elements inside each sub-array for RHCP and LHCP radiation and corporate feeding among the four sub-arrays. The signals in the low-frequency and high-frequency bands were separated using a diplexer made of microstrip open ring resonators and substrate integrated

multimode resonators directly coupled to the patch elements. The measured results of the prototype show an S_{11} < -10 dB bandwidth of 7.2–7.75/7.85–8.4 GHz, an AR < 3 dB bandwidth of 7.4–7.7/7.95–8.32 GHz, and a gain of 14/14.2 dBic at the low/high-frequency bands (see Figure 2(b)). The measured channel isolation is more than 27 dB while the sidelobe levels are below −15 dB in both bands [11].

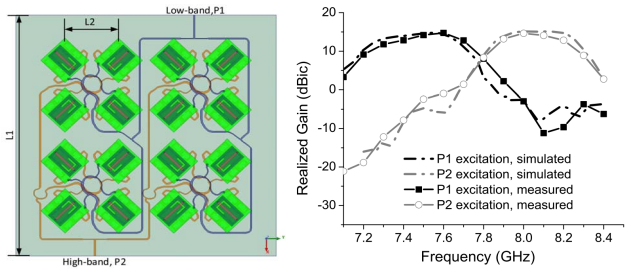

(a) (b)

Figure 2. (a) Configuration of the dual-port dual-CP self-diplexing *C*-band antenna array. (b) Simulated and measured realized gain of the LHCP and RHCP beams.

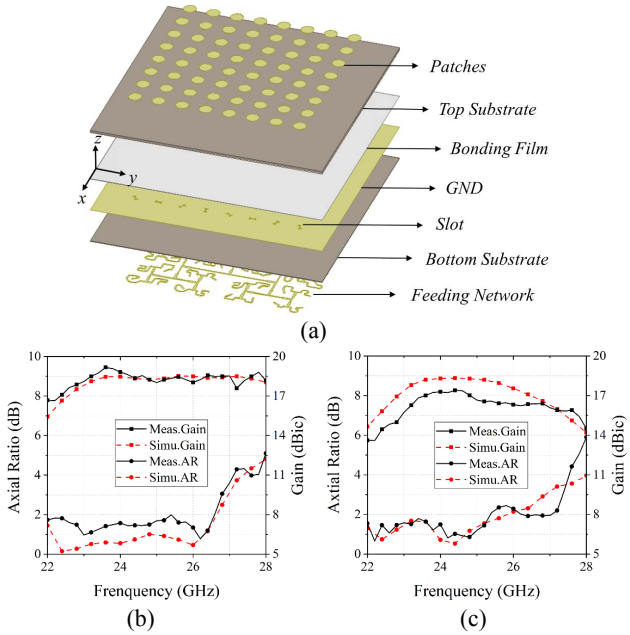

(a) (b) (c)

Figure 3. (a) Configuration of the single-port dual-CP dual-beam *K*-band antenna array. Simulated and measured AR and gain of the (b) LHCP and (c) RHCP beams.

The shortcoming of these sequential rotation arrays using LP elements or sub-arrays is that a single set of feeding network can only support CP radiated waves with a single handedness, leading to a peak aperture efficiency of only 50%. This is because at the same time these LP elements are aligned in a sequentially rotated arrangement, their feeding phases also need to follow the phase progression in correlation with the element rotation angles. Recently, we generalized the sequential rotation array technique such that an array of LP elements with a single feeding network can generated both LHCP and RHCP beams with independent beamforming capability. This is achieved by breaking the correlation between the element rotation angles and feeding phases. As shown in Figure 3(a), the single-feed dual-CP dual-beam array consists of an array of aperture-coupled LP circular patches with different orientations. On the bottom, the feeding network provides excitation phases for the patch arrays. The element rotation angle and feeding phase distributions jointly enable the RHCP and LHCP beams to point at (θ_R, ϕ_R) = (30°, 90°) and (θ_L, ϕ_L) = (20°, 0°), respectively. As shown in Figures 3(b) and 3(c), both the RHCP and LHCP beams possess a wide AR < 3 dB and 2-dB gain bandwidth at around 24 GHz [12].

3 Dual-CP RAs/TAs

The Dual-CP antenna arrays can accomplish either single-port or dual-port dual-CP radiation, however, as the array size increases, the gain enhancement due to the increased array elements will be quickly consumed by the loss in the expanded feeding network. Therefore, to obtain high-gain dual-CP beams, quasi-optical devices such RAs and TAs can be employed which possess much less loss since the power dividing process is achieved via propagating waves in free space. In order to design dual-CP RAs/TAs with a single-functional-layer, the rotational and dynamic phases need to be employed simultaneously. Different from the rotational phase used in sequential rotation antenna arrays, where the spin-dependent CP phase delay is equal to the rotation angle, here, the amount of CP phase delay is equal to twice the rotation angle of the RA/TA elements.

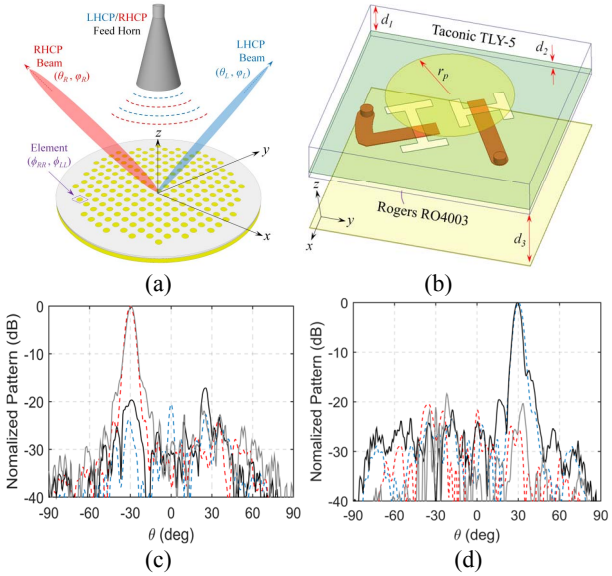

(a) (b) (c) (d)

Figure 4. (a) Configuration and (b) unit cell of the dual-CP *Ka*-band RA. Simulated and measured patterns in the *y*-*z* plane with a (c) LHCP and (d) RHCP feed at 30 GHz. Dashed red lines: simu. LHCP, solid grey lines: meas. LHCP, dashed blue lines: simu. RHCP, solid black lines: meas. RHCP.

As shown in Figures 4(a) and 4(b), the dual-CP RA is composed of an array of dual-LP aperture-coupled patch elements with a total thickness of about $0.3\lambda_0$. Underneath

each element, microstrip phase delay lines with different lengths were used to provide the dynamic phases. For each element, the two microstrip delay lines have a 180° phase difference such that the RA cell can provide a high co-polarized reflected wave for CP input waves. By introducing additional rotational phases into the element, dual-CP reflective phase delay with independent control of polarizations can be obtained. Consequently, when the RA is fed by a LHCP/RHCP horn, LHCP/RHCP high-gain beams can be generated each pointing at a specific direction. A prototype was fabricated and measured at the *Ka*-band. As displayed in Figures 4(c) and 4(d), directive LHCP and RHCP beams are achieved pointing at (θ_L, ϕ_L) = (-30°, 90°) and (θ_R, ϕ_R) = (30°, 90°), respectively. The measured peak gain values for the RHCP and LHCP beams are 28.4 and 28.3 dBic, while the measured joint 1-dB gain and AR < 2 dB bandwidths are about 16.0% and 14.7%, respectively [13]. More recently, this structure was extended into a dual-CP TA at around 20 GHz, exhibiting an operational bandwidth of about 16%.

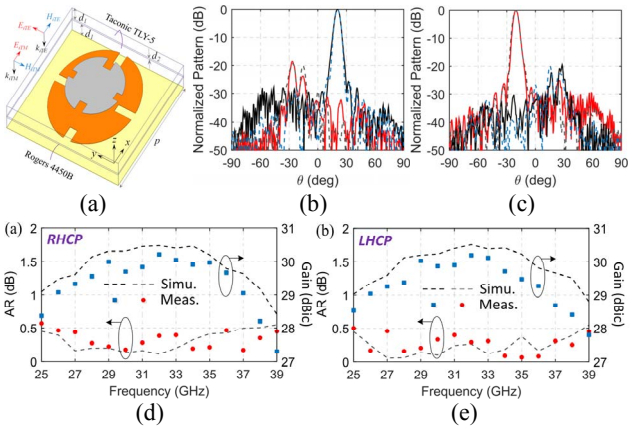

Figure 5. (a) Configuration of the dual-CP *Ka*-band RA cell. Simulated and measured patterns in the *x*-*z* plane with a (c) RHCP and (d) LHCP feed at 30 GHz. Dashed red lines: simu. LHCP, solid grey lines: meas. LHCP, dashed blue lines: simu. RHCP, solid black lines: meas. RHCP. Simulated and measured AR and peak gain of the (d) RHCP and (e) LHCP feed as a function of frequency.

In order to further enhance the bandwidth and reduce the profile of the dual-CP RA, a different structure was investigated based on multilayer anisotropic impedance surfaces. The RA cell is comprised by three metal layers – slotted two elliptical patches on the top and a metallic ground on the bottom (see Figure 5(a)), which can be analytically evaluated using a multilayer transmission line model. Through tailoring its anisotropic and dispersive scattering property, a much broader bandwidth than that of the dual-CP RA cell based on aperture-coupled patches can be obtained. As the simulated and measured pattern in the *x*-*z* plane shown (see Figures 5(b) and 5(c)), when the RA is fed by a RHCP or LHCP horn, a high-gain RHCP or LHCP beam can be obtained pointing at (θ_R, ϕ_R) = (-20°, 0°) and (θ_L, ϕ_L) = (20°, 0°), respectively. As displayed in Figures 5(d) and 5(e), the measured peak gain for the RHCP and LHCP beams are around 30.2 dBic [14]. The measured joint 1-dB gain and AR < 0.5 dB bandwidth is about 30% for RHCP and LHCP beams, which is slightly narrower than the simulation prediction.

4 Conclusions

In conclusion, we have presented in this summary recent development of dual-CP antenna arrays and RAs/TAs at microwave and millimeter-wave bands. Both these two kinds of dual-CP radiating devices utilize both rotational phases via element rotation and dynamic phases through phase shifters or resonators with variable sizes. The dual-CP array can find potential applications particularly for space communication systems.

6 Acknowledgements

The work is supported by National Natural Science Foundation of China (NSFC) under Grant 61801109.

7 References

1. S. Gao, Q. Luo, and F. Zhu, *Circularly Polarized Antennas*, Hoboken, NJ, USA: Wiley-IEEE Press, 2013.

2. T. M. Braun, *Satellite Communications Payload and System*, Hoboken, NJ, USA: Wiley-IEEE Press, 2012.

3. S. Cloude and E. Pottier, "A Review of Target Decomposition Theorems in Radar Polarimetry," *IEEE Transactions on Geoscience and Remote Sensing*, **34**, 2, March 1996, pp. 498-518, doi: 10.1109/36.485127.

4. R. R. Ramirez, F. De Flaviis and N. G. Alexopoules, "Single-feed Circularly Polarized Microstrip Ring Antenna and Arrays," *IEEE Transactions on Antennas and Propagation*, **48**, 7, July 2000, pp. 1040-1047, doi: 10.1109/8.876322.

5. J. Huang and J. A. Encinar, *Reflectarray Antennas*. New York, NY, USA: Wiley, 2008.

6. M. Maqsood *et al.*, "Low-cost Dual-band Circularly Polarized Switched-beam Array for Global Navigation Satellite System," *IEEE Transactions on Antennas and Propagation*, **62**, 4, April 2014, pp. 1975-1982, doi: 10.1109/TAP.2014.2301435.

7. J. Huang, "A Technique for an Array to Generate Circular Polarization with Linearly Polarized Elements," *IEEE Transactions on Antennas and Propagation*, **34**, 9, September 1986, pp. 1113-1124, doi: 10.1109/TAP.1986.1143953.

8. R. Deng, S. Xu, F. Yang, and M. Li, "An FSS-backed Ku/Ka Quad-band Reflectarray Antenna for Satellite Communications," *IEEE Transactions on Antennas and Propagation*, **66**, 8, August 2018, pp. 4353-4358, doi: 10.1109/TAP.2018.2835725.

9. Z. H. Jiang, L. Kang, T. Yue, W. Hong, and D. H. Werner, "Wideband Transmit-arrays Based on Anisotropic Impedance Surfaces for Circularly-polarized Single-feed Multibeam Generation in the Q-band," *IEEE Transactions on Antennas and Propagation*, **68**, 1, January 2020, pp. 217-229, doi: 10.1109/TAP.2019. 2943343.

10. J. Xu, W. Hong, Z. H. Jiang, J. X. Chen, and H. Zhang, "A Q-band Low-profile Dual Circularly Polarized Array Antenna Incorporating Linearly Polarized Substrate Integrated Waveguide Fed Patch Sub-Arrays," *IEEE Transactions on Antennas and Propagation*, **65**, 10, October 2017, pp. 5200-5210, doi: 10.1109/TAP.2017.2741065.

11. C. Mao, Z. H. Jiang, D. H. Werner, S. Gao, and W. Hong, "Compact Self-Diplexing Dual-band Dual-sense Circularly-polarized Array Antenna with Closely-spaced Operating Frequencies," *IEEE Transactions on Antennas and Propagation*, **67**, 7, July 2019, pp. 4617-4625, doi: 10.1109/TAP.2019.2911274.

12. R. F. Ma, Z. H. Jiang, Y. Zhang, T. Yue, W. Hong, and D. H. Werner, "Theory, Design, and Verification of Dual-circularly-polarized Dual-beam Arrays with Independent Control of Polarization: A Generalization of Sequential Rotation Arrays," under review

13. Z. H. Jiang, T. Yue, and W. Hong, "Low-profile and Wideband Dual-circularly-polarized Reflect-arrays Based on Rotated Metal-backed Dual-polarized Aperture-coupled Patch Elements," *IEEE Transactions on Antennas and Propagation*, 2019, early access, doi: 10.1109/TAP.2019.2948564.

14. Z. H. Jiang, Y. Zhang, and W. Hong, "Low-profile Anisotropic Impedance Surface Enabled Broadband Dual-circularly-polarized Multi-beam Reflect-arrays for Ka-Band Applications, *IEEE Transactions on Antennas and Propagation*, accepted, 2020.